Poynting vector and orbital angular momentum density of superpositions of Bessel beams

Igor A. Litvin,[1,3] Angela Dudley[1,2] and Andrew Forbes[1,2,*]

[1]*CSIR National Laser Centre, PO Box 395, Pretoria 0001, South Africa*
[2]*School of Physics, University of KwaZulu-Natal, Private Bag X54001, Durban 4000, South Africa*
[3]*ilitvin@csir.co.za*
[*]*aforbes1@csir.co.za*

Abstract: We study theoretically the orbital angular momentum (OAM) density in arbitrary scalar optical fields, and outline a simple approach using only a spatial light modulator to measure this density. We demonstrate the theory in the laboratory by creating superpositions of non-diffracting Bessel beams with digital holograms, and find that the OAM distribution in the superposition field matches the predicted values. Knowledge of the OAM distribution has relevance in optical trapping and tweezing, and quantum information processing.

OCIS codes: (050.0050) Diffraction and gratings; (050.4865) Optical vortices; (270.0270) Quantum Optics.

References and links

1. R. A. Beth, "Mechanical detection and measurement of the angular momentum of light," Phys. Rev. **50**(2), 115–125 (1936).
2. M. W. Beijersbergen, L. Allen, H. E. L. O. Van der Veen, and J. P. Woerdman, "Astigmatic laser mode converters and the transfer of orbital angular momentum," Opt. Commun. **96**(1-3), 123–132 (1993).
3. L. Allen, M. W. Beijersbergen, R. J. C. Spreeuw, and J. P. Woerdman, "Orbital angular momentum of light and the transformation of Laguerre-Gaussian laser modes," Phys. Rev. A **45**(11), 8185–8189 (1992).
4. J. Arlt and K. Dholakia, "Generation of high-order Bessel beams by use of an axicon," Opt. Commun. **177**(1-6), 297–301 (2000).
5. H. I. Sztul and R. R. Alfano, "The Poynting vector and angular momentum of Airy beams," Opt. Express **16**(13), 9411–9416 (2008).
6. H. He, M. E. J. Friese, N. R. Heckenberg, and H. Rubinsztein-Dunlop, "Direct observation of transfer of angular momentum to absorptive particles from a laser beam with a phase singularity," Phys. Rev. Lett. **75**(5), 826–829 (1995).
7. A. Mair, A. Vaziri, G. Weihs, and A. Zeilinger, "Entanglement of the orbital angular momentum states of photons," Nature **412**(6844), 313–316 (2001).
8. A. Vaziri, G. Weihs, and A. Zeilinger, "Experimental two-photon, three-dimensional entanglement for quantum communication," Phys. Rev. Lett. **89**(24), 240401 (2002).
9. J. T. Barreiro, T.-C. Wei, and P. G. Kwiat, "Beating the channel capacity limit for linear photonic superdense coding," Nat. Phys. **4**(4), 282–286 (2008).
10. J. Leach, B. Jack, J. Romero, A. K. Jha, A. M. Yao, S. Franke-Arnold, D. G. Ireland, R. W. Boyd, S. M. Barnett, and M. J. Padgett, "Quantum correlations in optical angle-orbital angular momentum variables," Science **329**(5992), 662–665 (2010).
11. G. Gibson, J. Courtial, M. J. Padgett, M. Vasnetsov, V. Pas'ko, S. M. Barnett, and S. Franke-Arnold, "Free-space information transfer using light beams carrying orbital angular momentum," Opt. Express **12**(22), 5448–5456 (2004).
12. S. N. Khonina, V. V. Kotlyar, R. V. Skidanov, V. A. Soifer, P. Laakkonen, and J. Turunen, "Gauss–Laguerre modes with different indices in prescribed diffraction orders of a diffractive phase element," Opt. Commun. **175**(4-6), 301–308 (2000).
13. G. C. G. Berkhout, M. P. J. Lavery, J. Courtial, M. W. Beijersbergen, and M. J. Padgett, "Efficient sorting of orbital angular momentum states of light," Phys. Rev. Lett. **105**(15), 153601 (2010).
14. J. Leach, M. J. Padgett, S. M. Barnett, S. Franke-Arnold, and J. Courtial, "Measuring the orbital angular momentum of a single photon," Phys. Rev. Lett. **88**(25), 257901 (2002).
15. C. Gao, X. Qi, Y. Liu, J. Xin, and L. Wang, "Sorting and detecting orbital angular momentum states by using a Dove prism embedded Mach–Zehnder interferometer and amplitude gratings," Opt. Commun. **284**(1), 48–51 (2011).
16. M. V. Vasnetsov, J. P. Torres, D. V. Petrov, and L. Torner, "Observation of the orbital angular momentum spectrum of a light beam," Opt. Lett. **28**(23), 2285–2287 (2003).

#146350 - $15.00 USD Received 21 Apr 2011; revised 2 Jun 2011; accepted 26 Jul 2011; published 15 Aug 2011

17. M. S. Soskin, V. N. Gorshkov, M. V. Vasnetsov, J. T. Malos, and N. R. Heckenberg, "Topological charge and angular momentum of light beams carrying optical vortices," Phys. Rev. A **56**(5), 4064–4075 (1997).
18. S. Franke-Arnold, J. Leach, M. J. Padgett, V. E. Lembessis, D. Ellinas, A. J. Wright, J. M. Girkin, P. Ohberg, and A. S. Arnold, "Optical ferris wheel for ultracold atoms," Opt. Express **15**(14), 8619–8625 (2007).
19. L. Paterson, M. P. MacDonald, J. Arlt, W. Sibbett, P. E. Bryant, and K. Dholakia, "Controlled rotation of optically trapped microscopic particles," Science **292**(5518), 912–914 (2001).
20. D. McGloin, V. Garcés-Chávez, and K. Dholakia, "Interfering Bessel beams for optical micromanipulation," Opt. Lett. **28**(8), 657–659 (2003).
21. K. Volke-Sepulveda, V. Garcés-Chávez, S. Chávez-Cerda, J. Arlt, and K. Dholakia, "Orbital angular momentum of high-order Bessel light beams," J. Opt. B Quantum Semiclassical Opt. **4**(2), S82–S89 (2002).
22. M. J. Padgett and L. Allen, "The Poynting vector in Laguerre-Gaussian laser modes," Opt. Commun. **121**(1-3), 36–40 (1995).
23. L. Allen and M. J. Padgett, "The Poynting vector in Laguerre-Gaussian beams and the interpretation of their angular momentum density," Opt. Commun. **184**(1-4), 67–71 (2000).
24. R. Zambrini and S. M. Barnett, "Angular momentum of multimode and polarization patterns," Opt. Express **15**(23), 15214–15227 (2007).
25. A. T. O'Neil, I. MacVicar, L. Allen, and M. J. Padgett, "Intrinsic and extrinsic nature of the orbital angular momentum of a light beam," Phys. Rev. Lett. **88**(5), 053601 (2002).
26. M. V. Berry, "Paraxial beams of spinning light," SPIE **3487**, 6–11 (1998).
27. L. W. Davis, "Theory of electromagnetic beams," Phys. Rev. A **19**(3), 1177–1179 (2003).
28. S. Orlov and A. Stabinis, "Propagation of superpositions of coaxial optical Bessel beams carrying vortices," J. Opt. A, Pure Appl. Opt. **6**(5), S259–S262 (2004).
29. S. Orlov, K. Regelskis, V. Smilgevicius, and A. Stabinis, "Propagation of Bessel beams carrying optical vortices," Opt. Commun. **209**(1-3), 155–165 (2002).
30. R. Vasilyeu, A. Dudley, N. Khilo, and A. Forbes, "Generating superpositions of higher-order Bessel beams," Opt. Express **17**(26), 23389–23395 (2009).
31. J. Durnin, J. Miceli, Jr., and J. H. Eberly, "Diffraction-free beams," Phys. Rev. Lett. **58**(15), 1499–1501 (1987).
32. J. Lin, X.-C. Yuan, S. H. Tao, and R. E. Burge, "Collinear superposition of multiple helical beams generated by a single azimuthally modulated phase-only element," Opt. Lett. **30**(24), 3266–3268 (2005).
33. M. Dienerowitz, M. Mazilu, and K. Dholakia, "Optical manipulation of nanoparticles: a review," J. Nanophoton. **12**, 1–32 (2008).
34. L. Torner, J. P. Torres, and S. Carrasco, "Digital spiral imaging," Opt. Express **13**(3), 873–881 (2005).
35. J. A. Rodrigo, A. M. Caravaca-Aguirre, T. Alieva, G. Cristóbal, and M. L. Calvo, "Microparticle movements in optical funnels and pods," Opt. Express **19**(6), 5232–5243 (2011).
36. S. H. Tao, X. C. Yuan, J. Lin, and R. E. Burge, "Residue orbital angular momentum in interferenced double vortex beams with unequal topological charges," Opt. Express **14**(2), 535–541 (2006).
37. C. H. J. Schmitz, K. Uhrig, J. P. Spatz, and J. E. Curtis, "Tuning the orbital angular momentum in optical vortex beams," Opt. Express **14**(15), 6604–6612 (2006).

1. Introduction

It has been well known for some time now that photons carry spin angular momentum of $+\hbar$ ($-\hbar$) per photon for left (right) circularly polarised light, and that the transfer of this momentum can be measured in the laboratory when the light passes through a birefringent plate [1]. More recently [2,3] it has been realised that light may also carry an extrinsic component of angular momentum, orbital angular momentum (OAM), when the electric field or mode has an azimuthal angular dependence of $\exp(il\varphi)$, where l is the azimuthal mode index. Such fields carry OAM of $l\hbar$ per photon, and may be found as beams expressed in several basis functions, including Laguerre-Gaussian beams [2], Bessel-Gaussian beams [4] and Airy beams [5] to name but a few. Since the discovery of light beams carrying OAM many new research areas have emerged, from transferring OAM to matter in optical tweezers [6] to investigating the conservation and entanglement of OAM in parametric down conversion for quantum information processing [7–11]. One of the problems has been the measurement of OAM, with various attempts at the efficient sorting of modes carrying OAM using interferometers and computer generated holograms [12–16]. Studies into the angular momentum of combined beams during free space propagation have also been made [17]. In general, one is interested in the superposition of OAM carrying fields, both at the classical [18–20] and quantum levels [7].

In this paper we consider the problem of calculating and then measuring the orbital angular momentum density of a coherent superposition of non-diffracting beams. We derive simple equations for the OAM density from first principles by calculating the Poynting vector of the field, and from this deduce both the linear and angular momentum components. The

#146350 - $15.00 USD Received 21 Apr 2011; revised 2 Jun 2011; accepted 26 Jul 2011; published 15 Aug 2011

results indicate that while the intensity pattern of the field is rotating at a fixed angular velocity (dependent on the relative phase velocities of the component fields), the OAM magnitude and direction is dependent on the location within the spatial distribution of the field. That is to say, different parts of the field carry different amounts of OAM, and of various sign. We verify the results by outlining and then executing a new technique for the direct measurement of the OAM density in the laboratory. We show how this approach allows for a quantitative measurement of the OAM spectrum as a function of position within the field.

2. Theory

We wish to consider the OAM density for a general complex scalar field, $u(x,y,z)$, which varies in time (in complex notation) as $\exp(i\omega t)$. This problem has been addressed by others previously [5,21–26], but with some inconsistencies in notation and derivation. For this reason, and for the benefit of the reader, we briefly outline the approach for defining OAM density, starting from the Poynting vector, before applying the result to the specific problem of coherent superpositions of non-diffracting Bessel beams. We start by defining a vector potential in the Lorentz gauge as a representation of our linearly polarized (in the x direction) laser mode as [27]:

$$\vec{A}(x, y, z) = u(x, y, z)\exp(i(kz - \omega t))\hat{x} \tag{1}$$

from which we can easily calculate the electric and magnetic field components of our complex scalar field:

$$\begin{aligned} \vec{B}(x, y, z) &= \nabla \times \vec{A}(x, y, z) \\ \vec{E}(x, y, z) &= \frac{ic^2}{\omega}\nabla \times \vec{B}(x, y, z), \end{aligned} \tag{2}$$

where $\vec{E}$ and $\vec{B}$ are the electric and magnetic fields of the laser mode, respectively, and all other terms have their usual meaning. Equations (2) can readily be solved to find the two fields as functions of the laser mode itself (our complex scalar field):

$$\begin{aligned} \vec{B}(x, y) &= ik\exp(i(kz - \omega t))\left(u(x, y, z)\hat{y} + \frac{i}{k}\frac{\partial u(x, y, z)}{\partial y}\hat{z}\right) \\ \vec{E}(x, y) &= i\omega\exp(i(kz - \omega t))\left(u(x, y, z)\hat{x} + \frac{i}{k}\frac{\partial u(x, y, z)}{\partial x}\hat{z}\right). \end{aligned} \tag{3}$$

Here we have applied the paraxial limit and assumed that the rate of change of the field in the z direction is small compared to the transverse directions to remove derivatives of the field in the z direction. We are now in a position to calculate the time average of the Poynting vector:

$$\vec{S} = \left\langle \vec{S}_{real} \right\rangle = \varepsilon_0 c^2 \left\langle \vec{E}_{real} \times \vec{B}_{real} \right\rangle, \tag{4}$$

where for brevity we will drop the arguments of the functions. The subscript *real* indicates that we are required to consider only the real part of the fields ($\cos(kz–\omega t)$), easily found to be:

$$\begin{aligned} \vec{E}_{real} &= \tfrac{1}{2}(\vec{E} + \vec{E}^*) \\ \vec{B}_{real} &= \tfrac{1}{2}(\vec{B} + \vec{B}^*), \end{aligned} \tag{5}$$

By substitution of Eqs. (3) and (5) into (4), and after removing all the oscillating terms since they average to zero (over time), one can show that

#146350 - $15.00 USD Received 21 Apr 2011; revised 2 Jun 2011; accepted 26 Jul 2011; published 15 Aug 2011

$$\begin{aligned}\vec{S} &= \varepsilon_0 c^2 \left\langle \vec{E}_{real} \times \vec{B}_{real} \right\rangle \\ &= \frac{\varepsilon_0 c^2}{4}\left(\vec{E}\times\vec{B}^* + \vec{E}^*\times\vec{B}\right) \\ &= \frac{\varepsilon_0 \omega}{4}\left(i\left(u\nabla u^* - u^*\nabla u\right) + 2k|u|^2\,\hat{z}\right),\end{aligned} \tag{6}$$

where it is understood that the gradient applies only in the transverse directions. We now wish to apply Eq. (6) to the problem of a superposition of OAM carrying fields, and we start with the problem of a coherent superposition of two such fields, of opposite handedness (i.e., opposite azimuthal phase), expressed in cylindrical co-ordinates as:

$$u(r,\varphi,z) = u_0(r,z)\exp(i\psi(r,z))\left(\exp(il\varphi) + \alpha_0\exp(-il\varphi)\right), \tag{7}$$

with the parameter α_0 representing the amplitude difference of the two fields (i.e., how the fields are weighted). The amplitude (u_0) and phase (ψ) of the complex scalar field is determined from the characteristics of the mode under study, and will be defined for Bessel and Bessel-Gauss beams a little later in this section. Substitution of Eq. (7) into Eq. (6) and solving for each component of the Poynting vector, we find that:

$$\begin{aligned}S_r &= \frac{\varepsilon_0\omega c^2}{2}\frac{\partial\psi}{\partial r}\left[u_0^2\left(1+\alpha_l^2+2\alpha_l\cos(2l\phi)\right)\right] \\ S_\phi &= \frac{-l\varepsilon_0\omega c^2 u_0^2}{2r}\left(\alpha_l^2-1\right) \\ S_z &= \frac{\varepsilon_0\omega c^2 k u_0^2}{2}\left(1+\alpha_l^2+2\alpha_l\cos(2l\phi)\right)\end{aligned} \tag{8}$$

In the case of a sum of Bessel and Bessel-Gaussian beams, the parameter $\alpha_l = \alpha_0(-1)^l$, whereas for Laguerre-Gaussian beams it takes the form $\alpha_l = \alpha_0$; here α_0 is the constant amplitude weighting of the fields. From these equations we may readily calculate the total angular momentum density of the field, and since by definition our field has a zero spin component, we have the total OAM density (along the direction of propagation, z) as:

$$L_z = \frac{1}{c^2}\left(r\times S\right)_z. \tag{9}$$

In this expression, the units of S are the conventional W/m^2, while the OAM density (L_z) is now expressed as the angular momentum per unit volume, or Ns/m^2. With these fundamentals in place, we are ready to calculate the OAM density for superposition fields.

2.1 Superposition of Bessel beams

Consider the general case of the superposition of two Bessel beams (BBs) of differing cone angles and opposite azimuthal phase; then Eq. (7) becomes

$$u(r,\phi,z) = A_0[J_l(q_1 r)\exp(i\Delta kz)\exp(il\phi) + \alpha_0 J_{-l}(q_2 r)\exp(-i\Delta kz)\exp(-il\phi)], \tag{10}$$

where J_l is the Bessel function of order l. Similar expressions can be found in references [28] and [29]. The cone angles, γ_1 and γ_2, differ as a result of the generation process (see later), but can be set to be equal if so required. As a result of the slightly different cone angles, both the radial and longitudinal wave numbers also differ for the two beams: the radial wave numbers become $q_i = k\sin\gamma_i$, while the longitudinal wave numbers, given by $k_i = k\cos\gamma_i$ differ from the central z-dependent wave number (k) by $\pm\,\Delta k$ (the subscripts i here refers to the first (second) beam in the superposition). We have maintained a normalization constant A_0 in order to later compare the theoretical results to experiment. Thus the Poynting vector becomes:

#146350 - $15.00 USD Received 21 Apr 2011; revised 2 Jun 2011; accepted 26 Jul 2011; published 15 Aug 2011

$$S_r = -\frac{A_0^2 \alpha_0 \varepsilon_0 \omega c^2}{2}\left[\left(q_2 J_{-l-1}(q_2 r) J_l(q_1 r) + q_1 J_{-l}(q_2 r) J_{l+1}(q_1 r)\right)\sin\left(2[l\phi + \Delta k z]\right)\right]$$

$$S_\phi = \frac{A_0^2 l \varepsilon_0 \omega c^2}{2r}\left(J_l^2(q_1 r) - \alpha_0^2 J_{-l}^2(q_2 r)\right) \tag{11}$$

$$S_z = \frac{A_0^2 \varepsilon_0 \omega c^2 k}{2}\left(J_l^2(q_1 r) + \alpha_0^2 J_{-l}^2(q_2 r) + 2\alpha_0 J_l(q_1 r) J_{-l}(q_2 r)\cos\left(2[l\phi + \Delta k z]\right)\right)$$

The time average Poynting vector, in both the r and z directions, has an additional term Δkz which is responsible for the slow rotation of the intensity distribution during its propagation. This behavior has been noted previously [30] and we can see that this is a result of the detuning of the radial wave numbers for the superposition of two or more beams. From the equation for S_r, a single non-diffracting beam has no S_r component. However, in the case of a superposition of two non-diffracting beams, the resulting beam has a non-zero S_r component. This results in a small rotation in the z direction, thus changing the intensity distribution of the superposition at a particular radial coordinate. We may easily then compute the OAM density to be:

$$L_z(r) = \frac{l \varepsilon_0 \omega A_0^2}{2}\left(J_l^2(q_1 r) - \alpha_0^2 J_{-l}^2(q_2 r)\right). \tag{12}$$

2.2 Superposition of Bessel-Gauss beams

Following a similar approach to that of section 2.1, we can find the OAM density for a superposition of two Bessel-Gauss beams (BGBs) of differing cone angles and opposite azimuthal phase, defined as

$$u(r,z,\phi) = \left(\frac{1}{\sqrt{1+(z/z_r)^2}}\right)\exp\left[\left(\frac{ik}{2z\left(1+(z/z_r)^2\right)} - \frac{1}{w_0^2\left(1+(z/z_r)^2\right)}\right)\left(r^2 + \gamma^2 z^2\right)\right]$$
$$\times\left(J_l\left(\frac{q_1 r}{1+i(z/z_r)}\right)\exp(ik_{z1}z)\exp(il\phi) + \alpha_0 J_{-l}\left(\frac{q_2 r}{1+i(z/z_r)}\right)\exp(ik_{z2}z)\exp(-il\phi)\right)\chi(z), \tag{13}$$

where we assume both fields are modulated by the same Gaussian beam of width w_0, resulting in a Gaussian Rayleigh range of z_r, and for brevity we have collapsed the phase terms related to the piston and Gouy phase shifts into the function $\chi(z)$. We may easily then compute the OAM density to be:

$$L_z(r,z) = \frac{l\varepsilon_0\omega}{2[1+(z/z_r)^2]}\times$$
$$\exp\left(-2\frac{r^2+\gamma^2 z^2}{w_0^2\left(1+(z/z_r)^2\right)}\right)\left[\left|J_l\left(\frac{q_1 r}{1+i(z/z_r)}\right)\right|^2 - \alpha_0^2\left|J_{-l}\left(\frac{q_2 r}{1+i(z/z_r)}\right)\right|^2\right]. \tag{14}$$

These results are consistent with what might be expected using the more general formalism of ref [24], and by extension of the vectorial results in ref [21]. Indeed, our results here are the special case of these two approaches for scalar fields (linear polarized) and where the superposition is due to interference of the two modes. It remains then to define a method of actually measuring this quantity in the laboratory, a subject that has not been adequately addressed to date.

#146350 - $15.00 USD Received 21 Apr 2011; revised 2 Jun 2011; accepted 26 Jul 2011; published 15 Aug 2011

2.3 Measuring the OAM density

Much attention has been paid to the measurement of OAM recently [12–16]. It is well known that since the angular harmonics, $\exp(il\varphi)$, are orthogonal over the azimuthal plane, we may express our superposition field in terms of such harmonics:

$$u(r,\phi,z)=\frac{1}{\sqrt{2\pi}}\sum_{l}a_l(r,z)\exp(il\phi), \tag{15}$$

with

$$a_l(r,z)=\frac{1}{\sqrt{2\pi}}\int_0^{2\pi}u(r,\varphi,z)\exp(-il\varphi)d\varphi. \tag{16}$$

The relative weighting of the power contained in each azimuthal mode can then be defined as [5]:

$$P_l(z)=\frac{\int_0^{\infty}\left|a_l(r,z)\right|^2 rdr}{\sum_l\int_0^{\infty}\left|a_l(r,z)\right|^2 rdr}. \tag{17}$$

From the definition of Eq. (16), one can easily show that the weighting of each harmonic for the case of a superposition of BBs is related to the OAM density through the relation:

$$L_z(r)=\frac{l\varepsilon_0\omega}{4\pi}\left(a_l^2(r)-a_{-l}^2(r)\right). \tag{18}$$

We will show, for the first time, how this quantity may be measured in the laboratory in an easy to implement procedure with a phase-only spatial light modulator (SLM), thus allowing a direct measurement of the OAM density of the light.

3. Experimental methodology

A HeNe laser (λ ~633 nm) was expanded through a 6 × telescope and directed onto the liquid crystal display (LCD) of a SLM (HoloEye, PLUTO-VIS, with 1920 × 1080 pixels of pitch 8 μm and calibrated for a 2π phase shift at ~633 nm) depicted in Fig. 1. The first SLM (denoted as LCD 1) was programmed to produce various superposition fields using the concept of Durnin's ring-slit [31], but implemented digitally [29]. Other techniques to experimentally generate superpositions of helically-phased fields using a single LCD exist and have been implemented by others [32]. By addressing alternating sets of pixels on the SLM with phase values that are out of phase by π, resulting in the light reflected from the LCD being scattered from its initial propagation axis, we are able to make use of our phase-only SLM to represent the ring-slit (which would usually require an amplitude device or mask).

To create a superposition of two non-diffracting beams of opposite handedness, the ring-slit was programmed with two opposite azimuthal phases, and the resulting field Fourier transformed at the focal plane after L3, to produce the field described by Eq. (10). The phase pattern in the annular region was separated into two ring-slits, each possessing an azimuthal phase of equal order but opposite handedness (Fig. 2(a)). When the orders, $|l|$, of the two azimuthal phases were of equal but of opposite handedness, a 'petal'-structure was produced, where the number of 'petals' is denoted by $2|l|$ (Fig. 2(b) and (c)), as expected from theory [30]. The slight difference in radius of the two rings resulted in cone angles (defined as R/f with R the ring radius) of γ_1 = 0.0069 rad and γ_2 = 0.0075 rad, so that Δk ~42.8801 m^{-1}. Another consequence of the slightly differing ring areas (see Fig. 2(a)) is that the energy contained in the two Bessel beams is not equal. Since the illuminating Gaussian beam was measured to be of radius w = 13.29 mm on LCD 1, the energy contained in each ring could be computed, and the weighting coefficients found:

#146350 - $15.00 USD Received 21 Apr 2011; revised 2 Jun 2011; accepted 26 Jul 2011; published 15 Aug 2011

$$\alpha_0 = \sqrt{\int_{ring\,1} \exp(-2(r/w)^2) r dr \Big/ \int_{ring\,2} \exp(-2(r/w)^2) r dr}. \qquad (19)$$

The resulting images of our non-diffracting superposition field were captured on a CCD camera (Spiricon, LBA-FW-SCOR-7350115), and the objective and camera could be positioned on translation stages with an optical rail in order to investigate the propagation of the resulting field. Once recorded, the resulting superposition field was then magnified with a 10 × objective and directed to the second SLM (LCD 2) for executing the modal decomposition of Eq. (16). This was accomplished by executing an inner product of the incoming field with the match filter set to $\exp(il\varphi)$, for various l values, and for particular radial (r) positions on the field. There are two important aspects of this experiment: firstly, the detection is restricted to the origin of the resulting field after the Fourier transforming lens L4, and secondly, the r dependence of the coefficient a_l is found by implementing the match filter in the form of a narrow (20 pixels) annular ring of radius r.

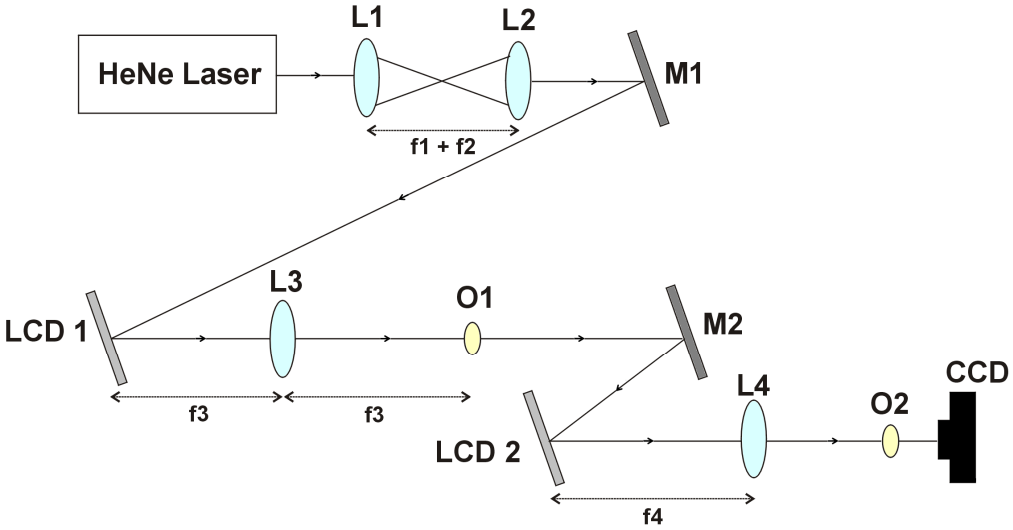

Fig. 1. A schematic of the experimental setup for detecting the OAM density of our superposition modes as a function of r. L: Lens (f1 = 25 mm; f2 = 150 mm; f3 = 200 mm and f4 = 200 mm); M: Mirror; LCD: Liquid Crystal Display; O: Objective; CCD: CCD Camera. The objective, O2, was placed at the focus (or Fourier plane) of lens, L4.

The latter requirement is necessary in order that we find the local OAM density rather than the global OAM density. Figure 3 illustrates the concept: the experimental field (Fig. 3; second and forth row) was subdivided radially into 10 sections, with each section sequentially apertured by an annular ring of width 20 pixels. The phase within the annular ring was varied according to the conjugate of the azimuthal modes in Eq. (15), i.e., the azimuthal integrand of Eq. (16), from –4 to + 4 in l index. Thus the decomposition of our field to find the weighting coefficients could be executed as a function of radial co-ordinate and azimuthal mode. This is the first time such a technique has been demonstrated experimentally, and allows for the OAM density to be measured directly: the OAM spectrum, $a_l(r,z)$ can be found at any radial position across the beam (and of course any z plane). The weighting parameter (α_0) of the superposition field was set by a suitable choice of the width of the two rings in the phase pattern on LCD 1: $\alpha_0 = 0.96$ (nearly equal weighting).

#146350 - $15.00 USD Received 21 Apr 2011; revised 2 Jun 2011; accepted 26 Jul 2011; published 15 Aug 2011

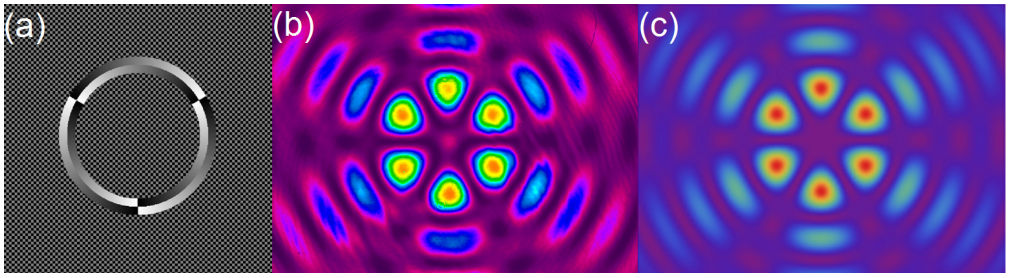

Fig. 2. (a) Annular ring programmed onto the SLM with two azimuthal phase patterns: in this example, + 3 and –3 l values; (b) observed experimental superposition (intensity) with 6 petals, and (c) the theoretically expected intensity pattern. The intensity shown in (b) is an attenuated experimental image with arbitrary false color units so as not to saturate the camera, while that in (c) shows a false color plot normalized to 1 in peak value for visual comparison.

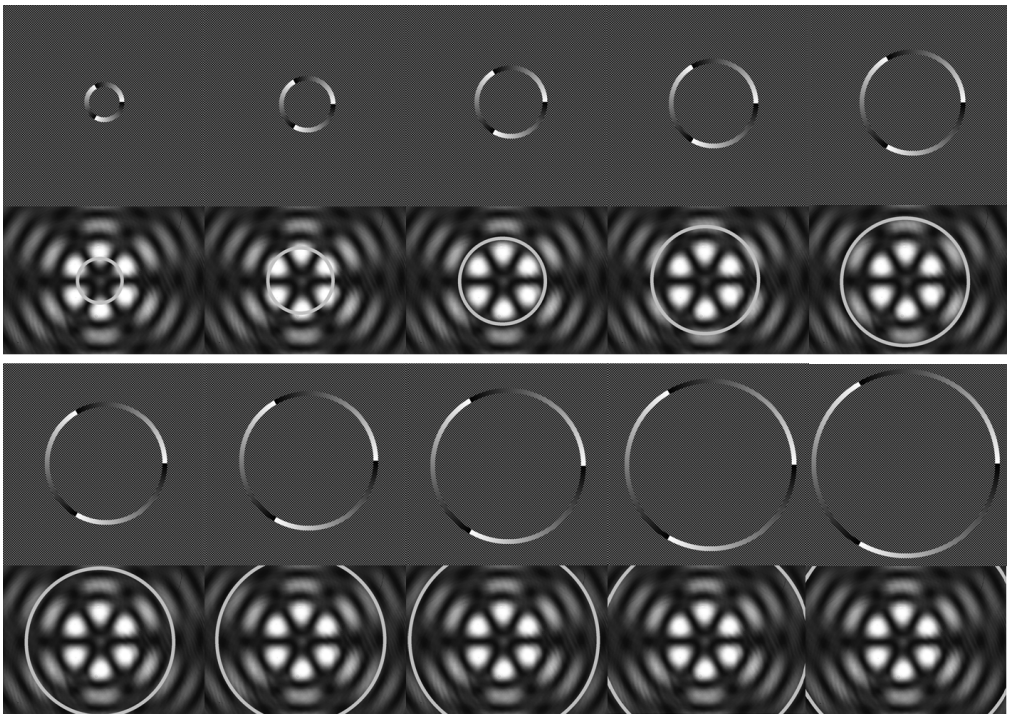

Fig. 3. The superposition field was divided radially, and an annular ring was programmed onto the second SLM in order to execute the inner product at only this radius. The phase within the annular ring was varied in the azimuthal angle for various values of l. The rest of the SLM was programmed with a checkerboard pattern so as to restrict the transmission function to the ring alone. The ten rings applied to LCD 2 have the following radii: r_1 = 600 μm, r_2 = 880 μm, r_3 = 1160 μm, r_4 = 1440 μm, r_5 = 1720 μm, r_6 = 2000 μm, r_7 = 2280 μm, r_8 = 2560 μm, r_9 = 2840 μm and r_{10} = 3120 μm. The black and white images in rows 2 and 4 are gray-scale experimental images of the beam, with the attenuation set so as not to saturate the camera. Therefore the intensity units are arbitrary.

Because of the manner in which the experiment was executed, by a Fourier transform evaluated at the origin to after the second SLM, the actual measured quantities are related to the OAM density by

$$L_z = \frac{l\omega}{\eta c}\left(\frac{\lambda f}{S_{ring}}\right)^2 \left(I_3(0) - I_{-3}(0)\right), \tag{20}$$

#146350 - $15.00 USD Received 21 Apr 2011; revised 2 Jun 2011; accepted 26 Jul 2011; published 15 Aug 2011

where $I_3(0)$ and $I_{-3}(0)$ are the measured signals on the CCD detector (see Fig. 1), f is the focal length of the final Fourier transforming lens, and S_{ring} is the area of the annular ring on the 2nd SLM. The coefficient η is to account for the losses in the optical system, e.g., the efficiency of the SLM and attenuators prior to the camera, which in our experiments was typically 0.0032 (or 0.32%).

4. Results and discussion

Applying Eq. (12), we calculate the dependence of the OAM density of a superposition of BBs, where the two components differ in their radial wave numbers. In Fig. 4(a) we see the results for the case of a 633 nm laser beam in a superposition of + 3 and –3 BBs, where the cone angle of the + 3 beam is fixed at 0.5° (line A on the graph) and that of the –3 BB is varied from 0.4° to 0.6°. Two results are evident: firstly, if the cone angles of the two BBs differ, so that their radial wave numbers differ, then the OAM density changes sign as one moves radially across the field. Secondly, the oscillation in the OAM density can be made to change value (magnitude and sign) by changing the relative difference in the cone angles (see line B of Fig. 4(a)). This is due to the oscillating nature of the Bessel function, where the period of the oscillation depends on the radial wave number, and in this particular case we have a superposition of two oppositely oscillating functions having opposite signs for their angular momentum. This can be seen by considering line B on the graph (varying cone angles), where the OAM density changes from a large positive value to a large negative value as one considers a single ring in the field (single radial position), passing through a zero value in between. In the case that the two cone angles are equal and the amplitude of the two Bessel beams are equal, the resulting superposition carries no angular momentum (see line A of Fig. 4(a)).

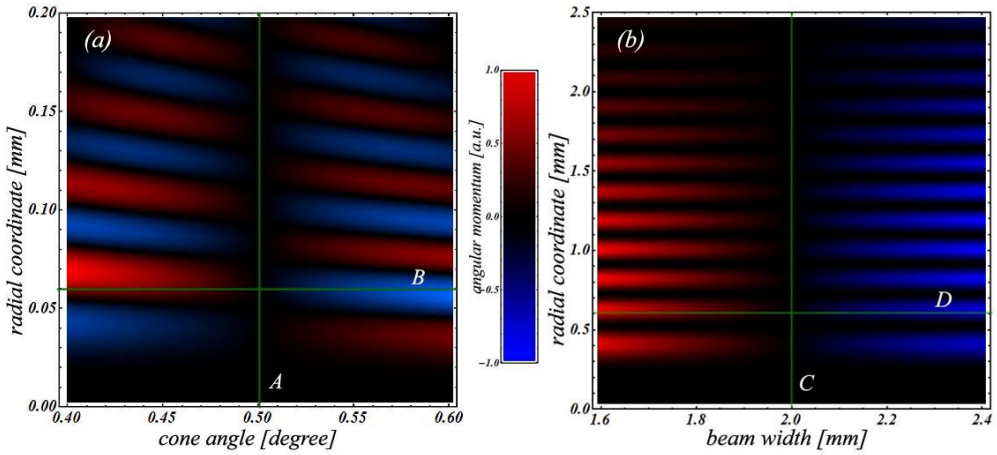

Fig. 4. Calculated change in the local OAM when (a) the cone angle of the two modes differ, and (b) when the weighting of the two modes differ.

Similarly for BGBs, Eq. (14), we calculate the dependence of the OAM density of a superposition of BGBs, where the two components differ in their weighting. In Fig. 4(b) we see the results for the case of a 633 nm laser beam in a superposition of + 5 and –5 BGBs, both having a cone angle of 0.5 °, but with various weightings of the two beams. Clearly even with equal phase velocities (Δk = 0) the OAM density can be engineered to be non-zero as long as the weighting of the two fields differ: the larger the difference, the greater the OAM density. By considering line D on the graph (varying weighting by varying the input Gaussian beam width), the OAM density changes from a large positive value to a large negative value as one considers a single ring in the field (single radial position), passing through a zero value in between. However for a given weighting of the two fields, as one moves radially across the field, so the OAM density remains either positive or negative (passing through nulls between

#146350 - $15.00 USD Received 21 Apr 2011; revised 2 Jun 2011; accepted 26 Jul 2011; published 15 Aug 2011

the rings), but does not oscillate in sign as in the case of Fig. 4(a). The variations in the angular momentum, both in terms of sign and magnitude, results from the variations in the amplitude and cone angles of the superimposed Bessel beams (refer to Fig. 6(a) and (b)). The manipulation of the angular momentum can be implemented efficiently by the method described above and is a useful tool for the controlling of optical forces [33].

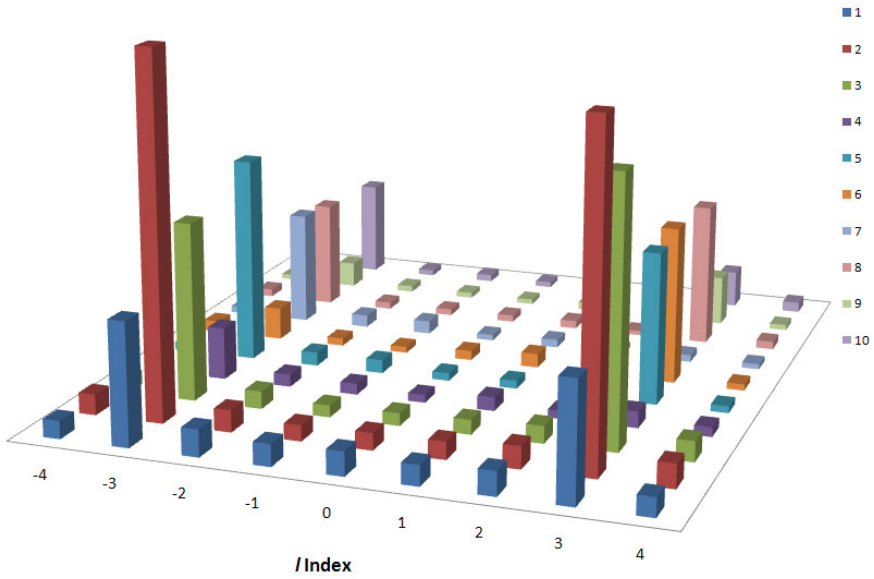

Fig. 5. The measured OAM spectrum (for l values of –4 to + 4) as a function of the radial ring on the beam (equivalent to the radial position on the beam), from 1 to 10, given by: r_1 = 600 µm, r_2 = 880 µm, r_3 = 1160 µm, r_4 = 1440 µm, r_5 = 1720 µm, r_6 = 2000 µm, r_7 = 2280 µm, r_8 = 2560 µm, r_9 = 2840 µm and r_{10} = 3120 µm. The height of each bar represents the measured coefficients $|a_l|^2$.

The predicted OAM density was measured in the laboratory by measuring directly the coefficients given by Eqs. (16) and (17), with the OAM density calculated from Eq. (20). The measured OAM spectrum for the equally weighted superposition beam is shown in Fig. 5

From the spectrum in Fig. 5, the OAM density could be inferred directly and compared to theory, with the results shown in Fig. 6. In Fig. 6 (a) and (b) we see a density plot of the two fields (for + 3 and –3), and the slight shift in rings is evident due to the slightly different radial wave numbers of the two fields. The superposition field is shown in Fig. 6 (c). In all three plots the measured radial positions (r_1 through r_{10}) are overlaid as vertical lines. The core result is Fig. 6 (d), where the analytical OAM density prediction (solid curve) as a function of the radial position on the superposition field is shown with the measured OAM density (red bars). It is very clear that there is excellent quantitative agreement between the two (with the exception of the first measurement radius which appears to have a large error). This agreement can also be noted by considering Fig. 6 (e) and (f), where the theoretical and experimental data are shown for the $|a_3|^2$ and $|a_{-3}|^2$ coefficients as a function of the radial position on the beam.

It should be noted that this is the first direct measurement of the OAM density, or OAM spectrum, to date. The importance of measuring the spectrum has been pointed out by others, where knowledge of the spectrum or local OAM is critical for imaging [34] and optical funnels [35], but the few measurements of the OAM either only consider the global OAM using an optical trapping set-up [36,37], or are unduly complicated by making use of Doppler shifts in due to a rotating detector [16]. In the method proposed here, the same principles (and optical elements) applied in creating the superposition fields can be used to decompose them.

#146350 - $15.00 USD Received 21 Apr 2011; revised 2 Jun 2011; accepted 26 Jul 2011; published 15 Aug 2011

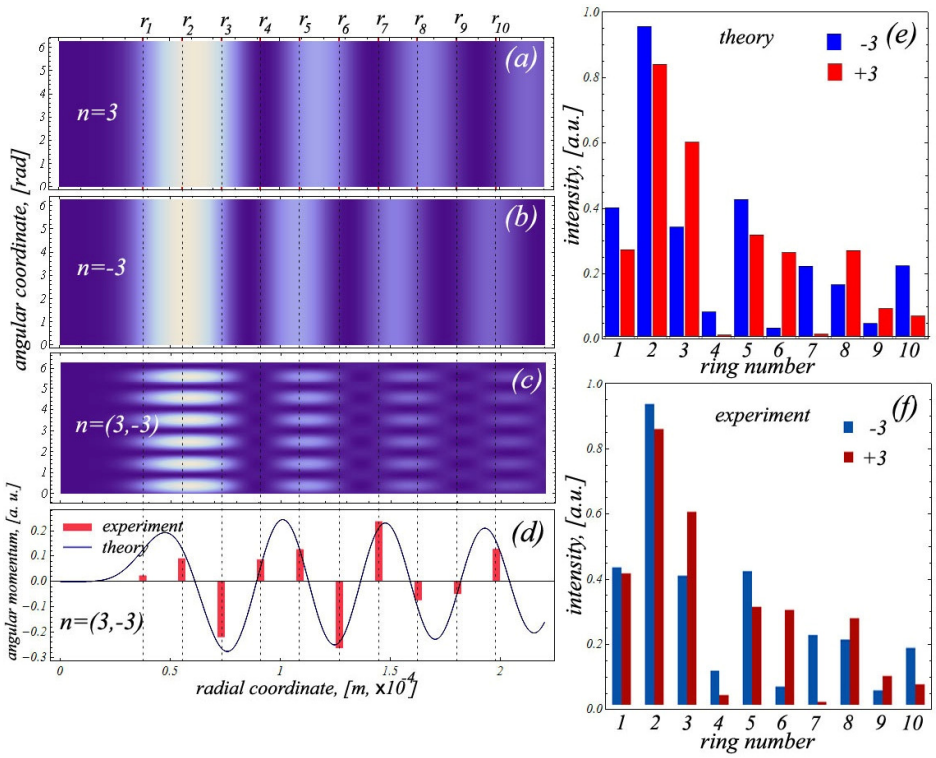

Fig. 6. (a) – (c): Density plots of the three Bessel beams plotted as (r,ϕ) for the + 3 case, the –3 case, and the superposition, respectively; (d) plot of the orbital angular momentum density as a function of radial position on the field – the theory is the solid curve and the experimental data is overlaid as red bars; (e) theoretical prediction of the coefficient $|a_l|^2$ (or the on axis intensity of the inner product) as a function of the radius of the match filter. Rings 1 to 10 denote those given in the first and third rows of Fig. 3; (f) corresponding experimental data.

It is interesting to consider the role of the Gouy phase shift in such measurements, since in general this is a function of the azimuthal order of the field. This is not the case for a superposition of Bessel beams, as reported here, and so may be neglected. However, in the case of Laguerre-Gaussian modes (which are used extensively in quantum information studies) the Gouy phase shift would be identical for fields of opposite handedness, proportional to $2p + |l| + 1$, where p is the radial order. This means that modes of $+ l$ and a $-l$ will have the same phase shift, so again it can be considered as a constant phase offset (but dependent on z). However, while the OAM arises from the azimuthal phase variation, the rotation of the Poynting vector is equal to $\arctan(z/z_r)$ when considering the radius of maximum field of $p = 0$, $l \neq 0$ modes (since such modes are a single ring of light), i.e., the rotation looks like the Gouy phase shift of a Gaussian mode. The salient point is that the Poynting vector rotation is proportional to $\arctan(z/z_r)$, and that the maximum rotation is fixed, in the case of a $p = 0$ mode, to $\pi/2$ either side of the beam waist. As the radial order is increased, so the maximum rotation of the field also increases [22,23]. It is however interesting to consider what happens to the OAM density if non-zero radial modes are excited, as will surely be the case for the typical laboratory practices of generating such modes by multiplication of a Gaussian with a purely azimuthal phase function. This case has not yet been treated fully in the literature. The result would, most likely, be a superposition not only in l but also in p, resulting in an OAM spectrum with weighting coefficients different to that of a purely azimuthal superposition, with a larger contribution from the a_0 term in Eq. (16) due to the azimuthal symmetry of the radial orders.

#146350 - $15.00 USD Received 21 Apr 2011; revised 2 Jun 2011; accepted 26 Jul 2011; published 15 Aug 2011

5. Conclusion

We have used the Poynting vector approach to study the OAM density within fields that are superpositions of non-diffracting Bessel and Bessel-Gauss beams. We find that while the global OAM is zero, the local OAM spectrum changes radially across the beam, and can be made to oscillate from positive to negative values by a suitable choice of the parameters making up the superposition (e.g., relative phase velocity of the two component beams). The implication is also that in applications such as optical trapping with so-called bottle beams and optical funnels, the rotating intensity distribution may also carry OAM that varies across the beam in a predictable but non-negligible manner. We have demonstrated the theory by creating such superposition beams in the laboratory with a phase-only spatial light modulator, and have implemented a new technique for the direct measurement of the OAM density. Previous studies of such fields either remained purely theoretical, or have attempted to show the OAM component by demonstrating rotation within an optical trapping and tweezing system. Needless to say, the latter is not only an indirect measurement, but also a very difficult experiment to execute. The technique we outline here requires only an SLM and a lens, and is therefore easy to implement in the laboratory (anyone who is able to create the original fields is also now able with the same approach to measure the OAM density). Both the generation of the superposition fields, and the measurement of the OAM spectrum, have direct relevance in quantum studies of OAM entanglement, and classical studies of OAM transfer in optical trapping and tweezing systems.

#146350 - $15.00 USD Received 21 Apr 2011; revised 2 Jun 2011; accepted 26 Jul 2011; published 15 Aug 2011